JOURNAL OF
Materials
CHEMISTRY

IR laser-induced reactive ablation of silicon monoxide in hydrogen and water atmosphere

Vladislav Dřínek,[a] Zdeněk Bastl,[b] Jan Šubrt,[c] Akira Yabe[d] and Josef Pola*[a]

[a]*Institute of Chemical Process Fundamentals, Academy of Sciences of the Czech Republic, 165 02 Prague, Czech Republic*
[b]*J. Heyrovský Institute of Physical Chemistry, Academy of Sciences of the Czech Republic, 182 23 Prague, Czech Republic*
[c]*Institute of Inorganic Chemistry, Academy of Sciences of the Czech Republic, 25068 Řež near Prague, Czech Republic*
[d]*National Institute of Materials and Chemical Research, AIST, MITI, Tsukuba, Ibaraki, 305, Japan*

Received 3rd January 2002, Accepted 4th April 2002
First published as an Advance Article on the web 26th April 2002

TEA CO_2 laser induced ablation of solid amorphous silicon monoxide in H_2 and H_2O atmosphere results in deposition of hydrogenated SiO_x films, which reveals that ablated silicon monoxide fragments are reactive towards H_2 and H_2O. The films analyzed by FTIR and XP spectroscopy are revealed as rich in H, composed of Si^0 and several $Si_xO_yH_z$ configurations and containing both Si–OH and Si–H bonds. The films produced in H_2O have (Si)H mostly bonded in the (O_3)Si–H unit and those produced in H_2 have H attached to Si which is bonded to 1–3 oxygen atoms.

Introduction

Silicon monoxide, SiO, is a well known gaseous species[1,2] that when condensed in inert gas cryogenic matrices undergoes fast polymerization,[3,4] reactions with halogens,[5–7] organic compounds[8–10] and metals.[11–19]

The structure of solid silicon monoxide appears to depend on the conditions under which it has been formed from the gas phase. Its composition is close to SiO, if obtained in the total absence of oxygen.[20] Various models differ by the relative amounts of the tetrahedral $Si(Si_4)$, $Si(Si_3O)$, $Si(Si_2O_2)$, $Si(SiO_3)$ and $Si(O_4)$ units. Suggested structures are a "random bonding model" (a statistical mixture of Si–Si and Si–O bonds[21,22]), a homogeneous 1 : 1 mixture of small Si and SiO_2 particles, a mixed-phase model[23] in which nano-sized Si and SiO regions are connected by a region of intermediate stoichiometry, and a modified mixed-phase model with some regions rich in Si–Si and other regions rich in Si–O bonds.[24]

Conversely to the chemistry of the gaseous silicon monoxide, that of the solid form has been little studied; the solid SiO undergoes oxidation[25,26] to Si(IV) compounds, such as SiO_2, silicates, or $SiCl_4$, reacts[27] with aqueous HF to Si and polysilanes, it is degraded by alkaline glycolates to form pentacoordinated silicon compounds,[28] and can be reduced[24] by Mg to Mg_2Si.

UV laser ablation of solid SiO is believed[29] to result in disproportionation into Si and SiO_2. When conducted in oxygen, it yields SiO_2 films.[30,31]

Our examination of IR laser-induced ablation of solid SiO afforded[32] an SiO_x film whose structure was explained by a transfer of O atoms within the $Si(O_4)$, $Si(SiO_3)$, $Si(Si_2O_2)$, $Si(SiO_3)$ and $Si(Si_4)$ units to increase the contribution of the $Si(SiO_3)$ units.

In conjunction with our previous examinations on laser chemical vapour deposition of hydrogenated SiO_x films (*e.g.* refs. 33–35) we report in this work on IR laser-induced ablation of solid SiO in the presence of H_2 and H_2O vapours and on the chemical reactivity of the ablated species towards H_2 and H_2O. We also show that the method used is suitable for fabrication of broadly applied hydrogenated SiO_x films rich in hydrogen.

Experimental

IR laser ablation experiments were conducted in a vacuum deposition chamber (Fig. 1) which was first evacuated to 0.05 hPa by a rotary pump and containing hydrogen or water vapours at pressures of 10^{-1}–10^2 hPa and 5×10^{-1}–31 hPa, respectively. Lumps of silicon monoxide (Aldrich) were irradiated by pulses of a TEA CO_2 laser (Plovdiv University) operating with a frequency of 1 Hz on the P(20) line of the $00^01 \rightarrow 10^00$ transition (994.19 cm^{-1}). The laser pulse energy (0.15–0.80 J) and wavelength were measured using a pyroceramic detector (Charles University, a m1-1 JU model) and a CO_2 laser spectrum analyzer, respectively. The laser beam was focused at the SiO target and it induced silicon monoxide ablation along with deposition of films on a substrate (copper sheets, glass plates, KBr plates, 0.8 cm^2) housed in the chamber 4 cm from the SiO target. In a typical experiment, the amount of ablated SiO target amounted to tens of mg, whereas that of the deposited film on the substrate ranged between 0.1–0.5 mg.

The gaseous phase above the ablated target was analyzed by

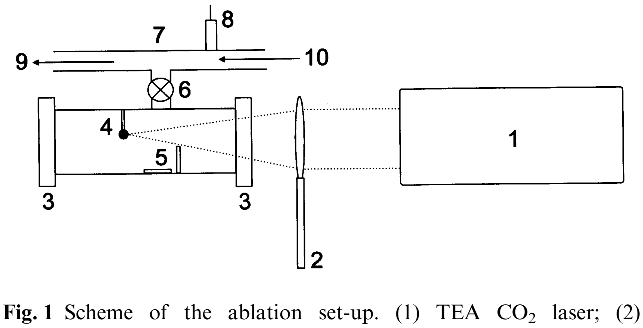

Fig. 1 Scheme of the ablation set-up. (1) TEA CO_2 laser; (2) germanium lens with 3D moving stage; (3) KBr windows; (4) holder with SiO target; (5) substrates; (6) valve; (7) vacuum line; (8) Pirani pressure gauge; (9) exhaust; (10) inlet for H_2O and H_2.

DOI: 10.1039/b200058j

gas chromatography (a Shimadzu GC 14A chromatograph) and on a Shimadzu model QP 1000 quadrupole mass spectrometer (ionizing voltage 70 eV), both equipped with Porapak P columns and programmed (20–150 °C) temperature. The deposition chamber was connected to a finger cooled with liquid nitrogen and the content of the finger was analyzed after admitting helium to atmospheric pressure by removing samples with a gastight syringe through a septum and passing them into the GC and GC/MS instruments.

Properties of the deposited films were analyzed by FTIR spectroscopy (a FTIR Nicolet Impact spectrometer), X-ray photoelectron spectroscopy and electron microscopy.

The FTIR spectral analysis was carried out on the films deposited on KBr sheets and deconvolution of the FTIR spectra in regions of 2100–2250 cm^{-1} and 800–1000 cm^{-1} was accomplished by using the Microcal Origin 4.1 program (Origin Lab. Corp., Northampton, USA). The absorbances for Si–H (stretching vibration at 2100–2300 cm^{-1}), Si–O (stretching vibration at 1060 cm^{-1}) and Si–OH (bending vibration at 1120 cm^{-1}) were determined by integration over the whole absorption peak.

The X-ray photoelectron spectra were recorded in an ESCA 310 (Gammadata Scienta) electron spectrometer equipped with a monochromatized AlKα source. The spectra were acquired at a pass energy of 300 eV with the sample surface normal to the analyzer electron optics. Peaks were fitted[36] using Gaussian/Lorentzian functions and Shirley background. The peak intensities were converted to elemental concentrations using theoretical values of photoionisation cross-sections.[37]

The SEM analyses were conducted on a Philips XL30 CP scanning electron microscope and TEM photomicrographs were obtained using a Philips 201 transmission electron microscope. In the latter case, the deposited materials were scraped from the substrate and transferred to a Formvar 1595 E (Merck) membrane coated Cu grid.

Results and discussion

Laser ablation of the dark brown silicon monoxide in the presence of H_2 and H_2O vapours yields light brown films which coat the substrates and nearby parts of the chamber. The search for gaseous/volatile products of the ablation process carried out by gas chromatography and GC/MS analysis did not reveal any volatile products.

FTIR spectra

The FTIR spectra of the solid films deposited on KBr sheets in atmospheres of H_2 (Fig. 2) and H_2O (Fig. 3) can be compared to that of the film produced by ablation of silicon monoxide in vacuum (Fig. 4, ref. 32). This comparison reveals that the FTIR spectral pattern of the former films is substantially different due to the modification of the shape and position of the ν(Si–O) band (above 1000 cm^{-1}) and the presence of new absorption bands due to Si–H vibrations (stretching mode at 2050–2300 cm^{-1} and deformation mode at 800–1000 cm^{-1}), Si–OH vibrations (bending modes above 900 cm^{-1}) and (Si)O–H vibrations (a broad band at 3500 cm^{-1}). The FTIR spectra thus provide clear evidence that the laser ablation of silicon monoxide in H_2 and H_2O results in chemical reactions of ablated species with molecules of H_2 and H_2O.

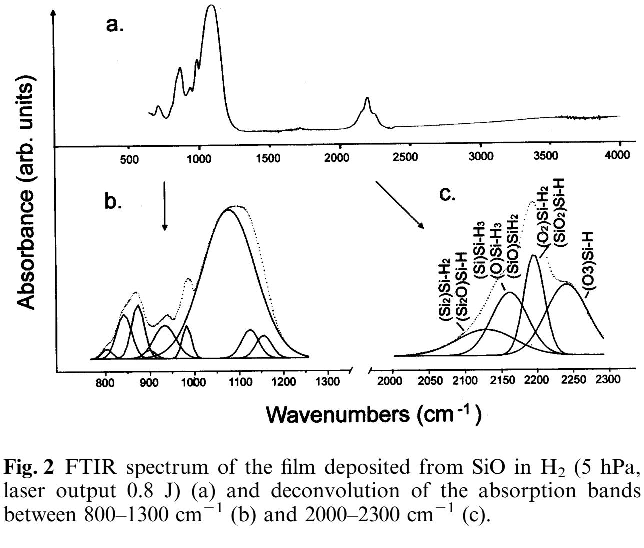

Fig. 2 FTIR spectrum of the film deposited from SiO in H_2 (5 hPa, laser output 0.8 J) (a) and deconvolution of the absorption bands between 800–1300 cm^{-1} (b) and 2000–2300 cm^{-1} (c).

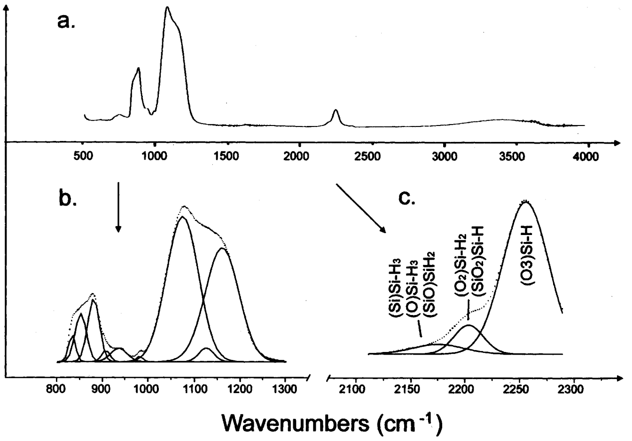

Fig. 3 FTIR spectrum of the film deposited from SiO in H_2O (5 hPa, laser output 0.8 J) (a) and deconvolution of absorption bands between 800–1300 cm^{-1} (b) and 2000–2300 cm^{-1} (c).

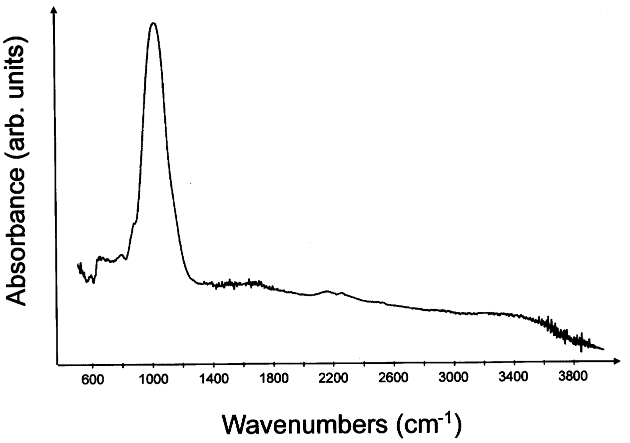

Fig. 4 FTIR spectrum of the film deposited by ablation of SiO in vacuum.

It is well known that the Si–H stretching mode is empirically related to the electronegativity/inductive effect of the neighbouring atoms[38,39] and that the H_nSi bending modes below 1000 cm^{-1} are less informative[40–43] of the structure of $SiO_x:H$ films.

The deconvolution of the bands between 2050–2300 cm^{-1} and 800–1000 cm^{-1} (Figs. 2 and 3) reveals that both regions are composed of the same number of peaks which were assigned, in agreement with the literature data, in Table 1. The absorption peak at 2250–2260 cm^{-1} relates to the (O_3)SiH configuration which has[47] its bending mode at 875 cm^{-1}. The peak at 2200 cm^{-1} is due to two configurations, the (SiO_2)SiH configuration typical in films with lower hydrogen content[38,47] and the (O_2)SiH_2 configuration[49] for which we detected the peaks at 940 and 980 cm^{-1} (ref. 39). The region between 2100 and 2200 cm^{-1} is known to be occupied by di- and trihydrido configurations. The peak with a maximum at 2140–2170 cm^{-1} possesses a very large full width at half maximum (FWHM), *ca.* 60 cm^{-1}, which suggests that it is composed of

Table 1 MH_x (M = Si, O) bands detected in SiO_x : H films[a]

Bonding configuration	Absorption band/cm^{-1} Ablation in H_2	 Ablation in H_2O	Reference
$(Si_2)SiH_2$; $(Si)SiH_3$; $(SiO_2)SiH$	840–854	841–849[b]	38,44,45; 44,46; 44,47
$(O_3)SiH$; $(Si)SiH_3$	868–877	877–882	39,44,47; 44,46
$(Si_2)SiH_2$; $(Si)SiH_3$	896–916	903–910	38,44,45,48; 44
$(O_2)SiH_2$, Si–OH	931–941	931–940	34,39,49; 50
$(O_2)SiH_2$	970–983	975–983	34,39
SiOH	1101–1120	1119–1150	38,41,43,50
$(Si_2)SiH_2$; $(Si_2O)SiH$	2083–2107	2114	38,43,44,45,48; 47
$(Si)SiH_3$; $(O)SiH_3$; $(SiO)SiH_2$	2150–2179	2163–2186	44,47; 34; 51
$(SiO_2)SiH$; $(O_2)SiH_2$	2193–2213	2203–2206	44,47; 34,39,49
$(O_3)SiH$	2246–2258	2252–2259	39,44,47

[a] Observed for H_2 (10^{-1}–10^2 hPa, 0.15, 0.3 and 0.8 J $pulse^{-1}$) and for H_2O (5×10^{-1}–31 hPa, 0.8 J $pulse^{-1}$). [b] 2 peaks at 834 and 855 cm^{-1} (5 hPa, 0.8 J).

Table 2 Comparison of absorbances of ν(Si–H) and ν(Si–O) bands

Film/compound	$A_{(\nu SiH)}/A_{(\nu SiO)}$	Method applied	Reference
SiO_x : H	0.1 (in H_2O or H_2)	ablation of SiO[a]	This work
$(H_2SiO)_4$	~0.5	—	52
SiO_x : H	~0.02	glow discharge in hexamethyldisiloxane	47
SiO_x : H	~0.02	SiO evaporation through glow discharge in hexamethyldisiloxane	53
SiO_x : H	~0.2	UV laser photolysis of disiloxane	33
SiO_x : H	~0.2	IR laser thermolysis of disiloxane	34

[a] Conditions: 5 hPa, 0.8 J $pulse^{-1}$.

sub-peaks. Deconvolution revealed the presence of $(Si_2)SiH_2$ and/or $(Si_2O)SiH$ configurations at 2100 cm^{-1} and is in line with other possible configurations—$(Si)SiH_3$, $(O)SiH_3$ and $(SiO)SiH_2$—having their absorptions under the 2140–2170 cm^{-1} peak.

It appears that the films produced in H_2 and H_2O are composed of the same configurations. However, the relative peak absorbances for the films obtained in both vapours (Figs. 2, 3) are different. In the films obtained in H_2O the peak of the $(O_3)SiH$ configuration prevails over those of the $(O_2)SiH_2$ + $(SiO_2)SiH$ and $(Si)SiH_3$ + $(O)SiH_3$ + $(SiO)SiH_2$ configurations. However, in the films obtained in H_2 these three peaks have almost equal absorbance.

These relative peak absorbances indicate that the films produced in H_2O have (Si)H mostly bonded in the (O_3)Si–H unit, whereas the films produced in H_2 contain H attached to Si which is bonded to 1–3 oxygen atoms.

The films deposited in H_2 and H_2O have similar $A_{(\nu SiH)} : A_{(\nu SiO)}$ ratios (0.11), but they differ in the relative absorbances of the δ(SiO–H) bands. The films deposited in H_2 and H_2O exhibit $A_{(\delta SiOH)} : A_{(\nu SiO)}$ ratios of 0.24 and 0.08 respectively. These values reveal that the formation of the Si–H bonds is feasible in both atmospheres, whereas the formation of the (Si)O–H bonds is more feasible in the presence of H_2.

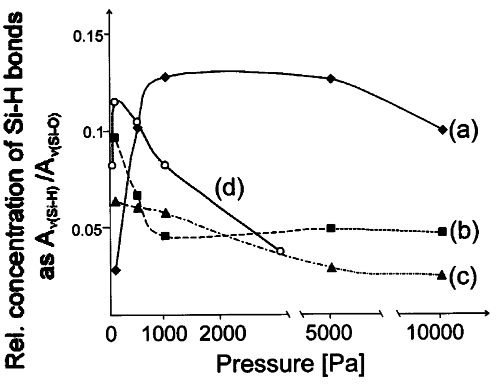

Fig. 5 Relative concentration of H(Si) *vs.* H_2 and H_2O pressure in films prepared in H_2 at 0.8 (a), 0.3 (b) and 0.15 (c) J and in H_2O at 0.8 J (d).

The extent of H incorporation into SiO can be estimated by comparing the $A_{(\nu SiH)}/A_{(\nu SiO)}$ ratios of the films to those in cyclotetrasiloxane and some SiO_x : H films produced by other techniques (Table 2). It is seen that the content of the Si–H bonds in the films prepared by the laser SiO ablation is dramatically higher than that in the films produced in plasmas[47,53] and somewhat lower than in the films obtained by laser chemical vapour deposition from disiloxane.

Ablation model

The $A_{(\nu SiH)} : A_{(\nu SiO)}$ and $A_{(\delta SiOH)} : A_{(\nu SiO)}$ ratios were used to estimate the dependence of the relative concentrations of H(Si) and H(O) atoms on the irradiating conditions (Figs. 5,6). It is seen that concentrations of both H(Si) and H(O) initially increase with higher pressure and later reach a plateau or slowly decrease. A later increase of the H(O) curves is noted

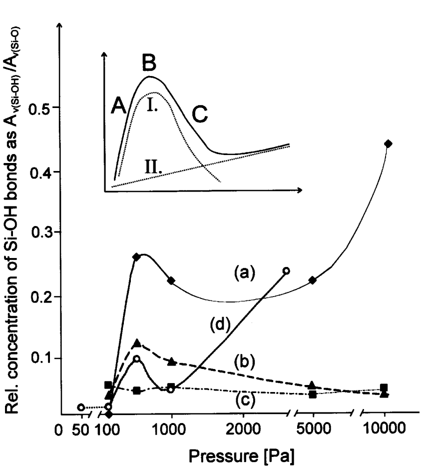

Fig. 6 Relative concentration of H(O) *vs.* H_2 and H_2O pressure in films prepared in H_2 at 0.8 (a), 0.3 (b) and 0.15 (c) J and in H_2O at 0.8 J (d). Inset – a model of the curve course.

Table 3 XPS and EDX analyses of the films[a]

XPS spectra					EDX analysis
Films deposited in	BE Si(2p)/eV	Percentage of state	Assignment[61–65]	Stoichiometry	Stoichiometry
H_2	99.5 ± 0.2	15 ± 5	Si^0	$Si_{1.00}O_{0.69}$	$Si_{1.00}O_{1.07}$
	100.8 ± 0.2	25 ± 3	H_3SiO		
	102.4 ± 0.2	60 ± 5	H_2SiO_2 and/or $HSiO_3$		
H_2O	99.7 ± 0.2	14 ± 2	Si^0	$Si_{1.00}O_{1.23}$	$Si_{1.00}O_{1.61}$
	102.1 ± 0.2	86 ± 5	H_2SiO_2 and/or $HSiO_3$		

[a]Conditions: 5 hPa, 0.8 J.

only for the ablation with the highest laser output (Fig. 6, curves a and d).

We can rationalize each curve as composed of a parabolic and linear function (inset in Fig. 6), each of them being due to different reaction phase, namely a plume propagating reaction phase (I) and a post-ablation reaction phase (II). In I, the front of the plume reacts with ambient gaseous molecules and is decelerated by them. At low gaseous pressures the deceleration is small, the ablated species deeply penetrate into the ambient atmosphere and undergo chemical reactions along their whole path towards the substrate (part A). At higher pressures, the plume deceleration is more important and the ablated species collide more in the plume volume, create clusters[54–56] and undergo fewer chemical reactions (part B). The mean free path in the gaseous atmosphere being shorter favours chemical reactions of the species on the plume surface. Further pressure increase enhances formation of larger clusters[57,58] and makes backward motion of ablated species possible.[54] In II, some reactive species undergo chemical reactions outside the propagating plume and the importance of these reactions increases with higher pressure (part C).

The discussion of the H(Si) and H(O) dependences on the H_2 and H_2O pressure using this model for the highest laser output is pertinent. The maximum of the H(Si) plot is at *ca.* 1 hPa for H_2O and between 10–50 hPa for H_2. The H(O) plot can be constituted by the parabolic and linear function, whereas the H(Si) plot can be described by the parabolic function only. This indicates that the H(O) centers are produced in both reaction phases and that the H(Si) centers are formed only in the plume propagating phase.

XPS spectra

X-Ray photoelectron spectra (XPS) of the Si (2p) electrons are a sensitive probe into the oxidation state of the Si atom and they show[59–61] large chemical shifts of the binding energy (BE) for Si^0, Si_2O, SiO, Si_2O_3 and SiO_2 states. The XPS study of the deposited films confirms (Table 3) that their topmost layers are composed[61–65] predominantly of Si^0 and H_3SiO, H_2SiO_2 and $HSiO_3$ configurations when the ablation takes place in H_2, and of Si^0 and H_2SiO_2 and (perhaps also $HSiO_3$) configurations when the ablation takes place in H_2O vapour. This method thus provides information on the presence of Si^0 that was reported[66,67] to be formed by heating of silicon monoxide.

The stoichiometry assessed for superficial layers of the films differs from that estimated for bulk films by EDX analysis (Table 3); the lower content of O at the surface can be explained by exposure of the samples for EDX analysis to the ambient air.

Electron microscopy

SEM images of the films deposited in the presence of H_2 and H_2O show similar morphology (Fig. 7a) consisting of aggregates whose sizes range from units to tens of μm. TEM analysis reveals particles of *ca.* 10 nm size and particles by at least 2 orders of magnitude larger (Fig. 7b); this indicates that the ablation process results in the formation of agglomerates with very different sizes.

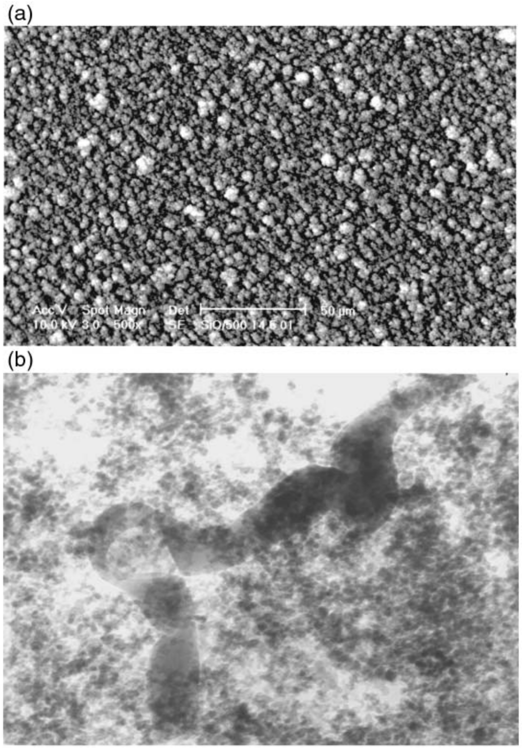

Fig. 7 SEM (bar 50 μm) of the deposit produced in H_2 (5 hPa) and TEM (magnification 100000 ×) of the deposit produced in the presence of H_2O (5 hPa).

Chemistry involved in reactive ablation of SiO

Chemical reactions of the ablated species with H_2 and H_2O molecules are apparently very complex. The IR laser-induced evaporation/ablation of SiO achieved through multi-photon resonant absorption of energy-poor infrared photons leads to high vibrational excitation of the solid[68,69] and can result in the formation of a variety of species such as silicon atoms, simple Si_xO_y transients, their clusters, as well as larger $(Si_xO_y)_n$ agglomerates, all of which are likely to contain reactive Si radical centers and/or Si=O bonds. The Si atoms/clusters can react with H_2 (ref. 70) and H_2O (ref. 71). Also the chemistry of SiO species with H_2 and H_2O has been theoretically predicted.[72,73] We can thus presume that Si-centered radical and/or Si=O bond containing species generated by the ablation react with H_2 and H_2O to yield various primary Si–H and Si–OH bonds containing products that undergo a myriad of further reactions, such as *e.g.* a H transfer from Si to O, intermolecular condensation regenerating H_2O and H_2, insertion reactions into Si–H, Si–O and H–H bonds, Si–H/Si–O scrambling, and polymerization. All these reactions have analogues in chemistry of molecules (1,2-H shift[73] in $H_2Si{=}O$, feasible H_2SiO polymerization,[74] insertion of $H_2Si{=}O$ into Si–O bonds,[75] insertion of H_2Si: into H–H and Si–H bonds,[76] and Si–H/Si–O redistribution[77,78]).

Conclusion

We have shown that the metastable silicon monoxide reacts with H_2 and H_2O molecules when ablated by intense pulses of infrared laser radiation and yields SiO_x : H films which are rich in H and contain both Si–H and SiO–H bonds.

Analysis of the films by FTIR and XP spectroscopy allowed them to be described as a mixture of Si^0 and several $Si_xO_yH_z$ configurations. FTIR analysis is in line with the films produced in H_2O having (Si)H mostly bonded in the $(O_3)Si–H$ unit and with the films produced in H_2 having H attached to Si which is bonded to 1–3 oxygen atoms. XPS analysis shows that the topmost layers are composed of Si^0 and H_3SiO, H_2SiO_2 and $HSiO_3$ configurations when the ablation takes place in H_2, and of Si^0 and H_2SiO_2 and $HSiO_3$ configuration when the ablation takes place in H_2O vapour.

The proposed ablation model involves two reaction phases, a plume propagating phase and a post-ablation phase. It is in line with the H(O) centers being produced in both reaction phases and with the H(Si) centers being formed only in the plume propagating phase.

Chemical reactions involved are judged to be analogous to those of Si atoms, silyl radicals, silylenes and silanones.

The reported method is promising for fabrication of organically modified inorganic materials, since the SiO_x : H films with Si–H and Si–OH bonds can be easily chemically modified by *e.g.* hydrosilylation and esterification reactions to yield organically modified materials that are now arresting so much attention (*e.g.* refs. 79–83).

Acknowledgement

The work was supported by the Grant Agency of the Czech Republic (grant no. 203/00/1288).

References

1 L. Brewer and K. Edwards, *J. Phys. Chem.*, 1954, **58**, 351.
2 R. F. Porter, W. A. Chupka and M. G. Inghram, *J. Chem. Phys.*, 1955, **23**, 216.
3 J. S. Anderson and J. S. Ogden, *J. Chem. Phys.*, 1969, **51**, 4189.
4 J. W. Hastie, R. H. Hauge and J. L. Margrawe, *Inorg. Chim. Acta*, 1969, **3**, 601.
5 H. Schnockel, *Angew. Chem., Int. Ed. Engl.*, 1978, **17**, 616.
6 H. Schnockel, *Z. Anorg. Allg. Chem.*, 1980, **460**, 37.
7 H. Schnockel, *J. Mol. Struct.*, 1980, **65**, 115.
8 E. T. Schaschel, D. N. Gray and P. L. Timms, *J. Organomet. Chem.*, 1972, **35**, 69.
9 S. R. Church, C. A. Cheetham, C. G. Davies, W. N. Rowlands and P. L. Timms, *Silicon for Chemical Industry*, ed. H. A. Oye and H. Rong, Geiranger, Norway, 1992.
10 W. N. Rowlands, A. D. Willson, P. L. Timms, B. Mile, J. H. B. Chenier, J. A. Howard and H. A. Joly, *Inorg. Chim. Acta*, 1991, **189**, 189.
11 A. P. Williams, R. J. Van Zee and W. Weltner, *J. Am. Chem. Soc.*, 1996, **118**, 4498 and references therein.
12 R. J. Van Zee, C. A. Baumann and W. Weltner, *J. Chem. Phys.*, 1985, **82**, 3912.
13 T. Mehner, H. Schockel, M. J. Almond and A. J. Downs, *J. Chem. Soc., Chem. Commun.*, 1988, 117.
14 J. H. B. Chenier, J. A. Howard, H. A. Joly, B. Mile and P. L. Timms, *J. Chem. Soc., Chem. Commun.*, 1990, 581.
15 T. Mehner, H. Schnockel, M. J. Almond and A. J. Downs, *J. Chem. Soc., Chem. Commun.*, 1988, 117.
16 R. Koppe and H. Schnockel, *Heteroatom. Chem.*, 1992, **3**, 329.
17 J. S. Anderson and J. S. Ogden, *J. Chem. Phys.*, 1969, **51**, 4189.
18 J. W. Hastie, R. H. Hauge and J. L. Margrave, *Inorg. Chim. Acta*, 1969, **3**, 601.
19 R. K. Kharma, D. D. Stranz and B. J. Donn, *J. Chem. Phys.*, 1981, **74**, 2108.
20 A. Songsasen and P. L. Timms, *J. Mater. Chem.*, 2000, **10**, 347.
21 H. R. Philipp, *J. Phys. Chem. Solids*, 1971, **32**, 1935.
22 H. R. Philipp, *J. Non-Cryst. Solids*, 1972, **8–10**, 627.
23 R. J. Temkin, *J. Non-Cryst. Solids*, 1975, **17**, 215.
24 E. Füglein and U. Schubert, *Chem. Mater.*, 1999, **11**, 865.
25 E. W. Zintl, W. Krings and W. Brauning, *US Patent* 2,242,497, 1941.
26 A. Weis and A. Weis, *Z. Anorg. Allg. Chem.*, 1954, **276**, 95.
27 P. L. Timms and C. S. G. Phillips, *Inorg. Chem.*, 1964, **3**, 606.
28 W. Donhärl, I. Elhofer, P. Wiede and U. Schubert, *J. Chem. Soc., Dalton Trans.*, 1998, 2445.
29 M. J. Godbole, D. H. Lowndes and A. J. Pedraza, *Appl. Phys. Lett.*, 1993, **63**, 3449.
30 E. Fogarassy, A. Slaoui, C. Fuchs and J. P. Stoquert, *Appl. Surf. Sci.*, 1990, **46**, 195.
31 E. Fogarassy, C. Fuchs, A. Slaoui and J. P. Stoquert, *Appl. Phys. Lett.*, 1990, **57**, 664.
32 V. Dřínek, J. Pola, Z. Bastl and J. Šubrt, *J. Non-Cryst. Solids*, 2001, **288**, 30.
33 J. Pola, M. Urbanová, Z. Bastl and H. Beckers, *J. Mater. Chem.*, 1999, **9**, 2429.
34 J. Pola, J. Pola, Z. Bastl, M. Urbanová, J. Šubrt and H. Beckers, *Appl. Organomet. Chem.*, 2000, **14**, 453.
35 J. Pola, M. Urbanová, V. Dřinek, J. Šubrt and H. Beckers, *Appl. Organomet. Chem.*, 1999, **13**, 655.
36 N. Fairley, CasaXPS Ver. 2.0.11, 2001.
37 J. H. Scofield, *J. Electron. Spectrosc. Relat. Phenom.*, 1976, **8**, 129.
38 G. Lucovsky, J. Yang, S. S. Chao, J. E. Tyler and W. Czubatyj, *Phys. Rev. B*, 1983, **28**, 3225.
39 D. V. Tsu, G. Lucovsky and B. N. Davidson, *Phys. Rev. B*, 1989, **40**, 1795.
40 F. L. Galeener and G. Lucovsky, *Phys. Rev. Lett.*, 1976, **37**, 1414.
41 G. Lucovsky, C. K. Wong and W. B. Pollard, *J. Non-Cryst. Solids*, 1983, **59/60**, 839.
42 G. Lucovsky, R. J. Nemanich and J. C. Knights, *Phys. Rev. B*, 1978, **18**, 4228.
43 W. B. Pollard and G. Lucovsky, *Phys. Rev. B*, 1982, **26**, 3172.
44 G. Lucovsky, R. J. Nemanich and J. C. Knights, *Phys. Rev. B*, 1979, **19**, 2064.
45 K. Luterova, I. Pelant, P. Fojtik, M. Nikl, I. Gregora, J. Kocka, J. Dian, P. Maly, J. Kudrna, J. Stepanek, A. Poruba and P. Horvath, *Philos. Mag. B*, 2000, **80**, 1811.
46 M. H. Brodsky, M. Cardona and J. J. Cuomo, *Phys. Rev. B*, 1977, **16**, 3556.
47 L. He, T. Inokuma, Y. Kurata and S. Hasegawa, *J. Non-Cryst. Solids*, 1995, **185**, 249.
48 E. C. Freeman and W. Paul, *Phys. Rev. B*, 1978, **18**, 4288.
49 M. Niwano, J. Kageyama, K. Kurita, K. Kinashi, I. Takahashi and N. Miyamoto, *J. Appl. Phys.*, 1994, **76**, 2151.
50 W. A. Pliskin and H. S. Lehman, *J. Electrochem. Soc.*, 1965, **112**, 1013.
51 D. Das and K. Barua, *Jpn. J. Appl. Phys. Part 2*, 1999, **38**, L697.
52 C. Fischer and H. Kriegsmann, *Z. Anorg. Allg. Chem.*, 1969, **367**, 219.
53 K. Kashiwagi, Y. Yoshida and Y. Murayama, *Jpn. J. Appl. Phys.*, 1991, **30**, 1803.
54 F. Kokai, K. Takahashi, K. Shimizu, M. Yudusaka and S. Ijima, *Appl. Phys. A*, 1999, **69**, 223.
55 F. Kokai, K. Takahashi, M. Yudusaka and S. Ijima, *J. Phys. Chem. B*, 2000, **104**, 6777.
56 Z. Paszti, G. Peto, Z. E. Horvath and A. Karacs, *Appl. Surf. Sci.*, 2000, **168**, 144.
57 T. Okada, J. Muramoto, Y. Nakada and M. Maeda, *Proceedings on the 4th Symposium on Photoreaction Control and Photofunctional Materials*, ed. M. Tachiya, H. Arakawa, T. Nakanaga, S. Murata, H. Sugihara, K. Kasuga, A. Yabe, N. Koshizaki, N. Minami, M. Matsumoto and I. Kojima, National Institute of Chemical Research (NIMC), Agency of Industrial Science and Technology, Ministry of International Trade and Industry (MITI), Japan, 2001, p. 74.
58 J. Muramoto, Y. Nakata, T. Okada and M. Maeda, *Appl. Surf. Sci.*, 1998, **127**, 373.
59 F. J. Himpsel, F. R. McFeely, A. Taleb-Ibrahimi, J. A. Yarmoff and G. Holliger, *Phys. Rev B*, 1988, **38**, 6084 and references therein.
60 M. Tabe, T. T. Chiang, I. Lindau and W. E. Spicer, *Phys. Rev. B*, 1986, **34**, 2706.
61 A. Namiki, K. Tanimoto, T. Makamura, N. Ohtake and T. Suzaki, *Surf. Sci.*, 1989, **222**, 530.
62 L. Yang, B. Abeles, W. Eberhardt and H. Stasiewski, *Phys. Rev. B*, 1989, **39**, 3801.

63 M. R. Alexander, R. D. Short, F. R. Jones, M. Stollenwerk, J. Zabold and W. Michaeli, *J. Mater. Sci.*, 1996, **31**, 1879.
64 H. Ogawa and T. Hattori, *Appl. Phys. Lett.*, 1992, **61**, 577.
65 A. Toneva, Z. Nenova, T. Marinova and V. Krastev, *Philos. Mag. A*, 1997, **75**, 331.
66 L. Brewer and R. K. Edwards, *J. Phys. Chem.*, 1954, **58**, 351.
67 R. C. Chittick, *J. Non-Cryst. Solids*, 1970, **3**, 255.
68 R. F. Haglund and D. R. Ermer, *Appl. Surf. Sci.*, 2000, **168**, 258.
69 L. V. Zhigilei, P. B. S. Kodali and B. J. Garrison, *J. Phys. Chem. B*, 1997, **101**, 2058.
70 e.g. (*a*) P. P. Gaspar, P. Markusch, J. D. Holten III and J. J. Frost, *J. Phys. Chem.*, 1972, **76**, 1352; (*b*) P. P. Gaspar, S. A. Bock and W. C. Eckelman, *J. Am. Chem. Soc.*, 1968, **90**, 6914.
71 Z. Kalafi Ismail, R. H. Hauge, L. Freidin, J. W. Kauffman and J. L. Margrave, *J. Phys. Chem.*, 1982, **77**, 1617.
72 M. R. Zachariah and W. Tsang, *J. Phys. Chem.*, 1995, **99**, 5308.
73 T. Kudo and S. Nagase, *J. Phys. Chem.*, 1984, **88**, 2833.
74 T. Kudo and S. Nagase, *J. Am. Chem. Soc.*, 1985, **107**, 2589.
75 G. Raabe and J. Michl, *Chem. Rev.*, 1985, **85**, 419.
76 J. M. Jasinski, R. Becerra and R. Walsh, *Chem. Rev.*, 1995, **95**, 1203.
77 V. Belot, R. J. P. Corriu, D. Leclercq, P. H. Muntin and A. Vioux, *J. Non-Cryst. Solids*, 1992, **144**, 287.
78 V. Belot, R. J. P. Corriu, D. Leclerque, P. H. Mutin and A. Vioux, *Chem. Mater.*, 1991, **3**, 127.
79 H. Cheng, R. Tamaki, R. M. Laine, F. Babonneau, Y. Chujo and D. R. Treadwell, *J. Am. Chem. Soc.*, 2000, **122**, 10063.
80 M. Okamoto, H. Abe, Y. Kusama, E. Suzuji and Y. Ono, *J. Organomet. Chem.*, 2000, **616**, 74.
81 T. Tao and G. E. Maciel, *J. Am. Chem. Soc.*, 2000, **122**, 318.
82 A. B. Sieval, R. Linke, H. Zuilhof and E. J. R. Sudholter, *Adv. Mater.*, 2000, **12**, 1457.
83 N. Y. Kim and P. E. Laibinis, *J. Am. Chem. Soc.*, 1997, **119**, 2297.